Machine Copy for Proofreading, Vol. x, y–z, 2011

A THREE-DIMENSIONAL TIME DOMAIN MICROWAVE IMAGING METHOD FOR BREAST CANCER DETECTION BASED ON AN EVOLUTIONARY ALGORITHM

M. Donelli[1, *], I. Craddock[2], D. Gibbins[2], and M. Sarafianou[2]

[1]Department of Information Engineering and Computer Science, University of Trento, Polo scientifico e tecnologico Fabio Ferrari, Via Sommarive 5, Trento, Italy

[2]Department of Electrical and Electronic Engineering, University of Bristol, Merchant Venturers Building, Woodland Road, Bristol, BS8 1UB, UK

Abstract—This paper presents a novel stochastic microwave method for the detection, location and reconstruction of electric properties of breast cancer in a simplified breast phantom. The method is based on the inversion of time domain data. The problem is recast as one of optimization by defining a suitable cost function which is then minimized using an efficient evolutionary algorithm. Selected numerical simulations of a simplified three dimensional breast model, and a realistic numerical phantom based on magnetic resonance images (MRIs) are carried out to assess the capabilities of the method. The results obtained show that the proposed method is able to reconstruct the properties of a tumor-like inclusion to a reasonable degree of accuracy.

1. INTRODUCTION

Breast cancer is one of the most common causes of death among women. The early detection of tumors and other tissues anomalies can potentially reduce mortality and increase the long term survival of patients and effectiveness of clinical treatments. X-ray mammography has an established role in breast cancer screening and diagnosis and has been shown to contribute to a reduction in breast cancer specific

Received 9 April 2011.

* Corresponding author: Massimo Donelli (massimo.donelli@disi.unitn.it).

mortality [1]. However, X-ray mammography performs badly in the radio graphically dense breast, typical of pre menopausal women. While other expensive diagnosis techniques such as contrast-enhanced breast magnetic resonance and positron emission tomography exist, cheaper methods for the screening of younger women, who are at risk for breast cancer, are desirable. In the last decade the use of medical microwave imaging has become a promising new technique for breast-cancer screening. Microwave imaging could be a valid supplement or alternative to X-ray mammography due the non-ionizing nature of microwave radiation and the superior electrical contrast at microwave frequencies. A number of different research groups have proposed microwave-based system prototypes for breast cancer detection [2–6] and a number of different active microwave imaging techniques are currently under development. In [7–11] ultra-wideband (UWB) radar imaging systems, based on the reflected UWB signals, have been proposed which determine the location of scatterers within the breast. Other approaches are aimed at the reconstruction of the complete dielectric properties of the breast tissues using a forward and inverse scattering models, based in both the frequency [12–14] and time domain [15–18]. In general the problems associated with microwave tomography are low resolution, the required a priori information, and the high computational resources required especially when three dimensional scenarios are considered. To solve the inverse problem, local searching techniques such as gradient based methods are usually considered to reduce the computational burden, but they can be trapped in local minima leading to false solutions. Global optimization techniques such as Genetic Algorithm (GA) [19, 20], Differential Evolution (DE) [21] and Particle Swarm Optimizer (PSO) [22, 23] can avoid the problem of local minima, but they can lead to a dramatic increase in the computational burden, as all of these imaging approaches require realistic numerical breast phantoms able to accurately model the geometrical properties of the breast, the inhomogeneities of the structure and the dispersive properties of the breast tissues. In this paper we describe a method for the detection, localization and reconstruction of unknown electrical characteristics (permittivity, and conductivity) of a cancer-like inclusion in a homogeneous breast phantom and in a realistic numerical phantom. We use scattered time domain data and the original inverse problem is recast as one of optimization by defining a suitable cost function. The cost function is then minimized using a stochastic evolutionary algorithm, known as the bee algorithm [24], avoiding the possibility of being trapped by local minima. To reduce the computational time a parallel implementation of the algorithm [25]

is used. The method is assessed by considering a simple three dimensional breast model and a realistic numerical phantom based on MRIs. The positions of the transmitting /receiving probes are chosen in order to accurately model the experimental prototype developed in [10]. The paper is structured as follows: after a general formulation of the time domain scattering problem reported (Section 2), the procedural schema of the proposed evolutionary algorithm is presented (Section 3). Section 4 reports some selected numerical simulations concerning a simple three-dimensional breast model and the MRIs based model. Finally in Section 5, conclusions are drawn and areas for future work are examined.

2. MATHEMATICAL FORMULATION

Let us consider the three dimensional model of human breast shown in Figure 1. The breast is represented as a hemisphere of radius R_b, and the chest of the patient with a tissue layer of thickness T_c. The breast is surrounded by 31 probes which can act as transmitters or as receivers. The breast is illuminated with a wide band pulse transmitted by one of the probes, while the measured field is collected by the remaining 30. The topology of the array mimics the experimental system developed by [4]. We assume the breast is immersed in a coupling liquid which completely fills the investigation scenario. The

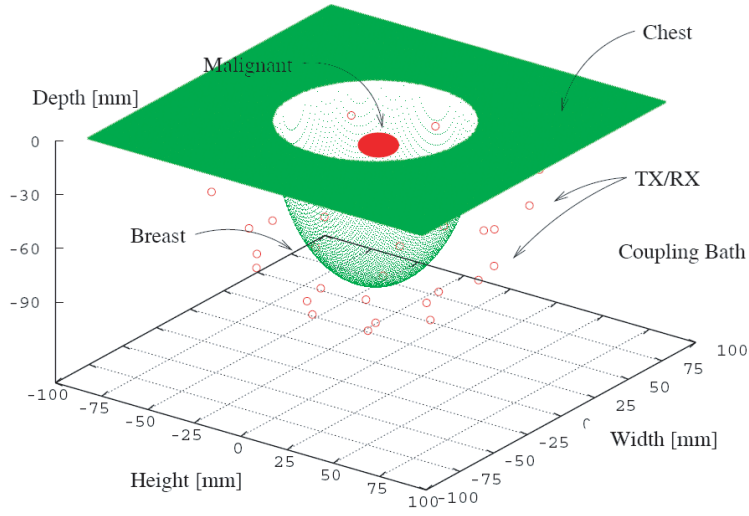

Figure 1. The three dimensional hemispherical breast model.

goal of the method is to reconstruct the characteristics of the malignant tissue namely the position of the center, the diameter and the electric characteristics starting from the time domain scattered field collected at the receiving probes. A transmission line matrix TLM solver [26] is used to produce synthetic measured and trial data. To apply the stochastic optimization method and solve the above inverse scattering problem, a cost function has to be formulated to estimate the errors between the scattering data, obtained from the actual configuration and the trial solution. The following relation represents the simplest expression for the error functional equation:

$$\Phi(\underline{x}) = \int_{t=0}^{T} \sum_{g=1}^{G} \sum_{r=1}^{R} \frac{\left| E_{g,r}^{(z)}(\underline{x}, t) - E_{g,r}^{(z),act}(t) \right|^2}{\left| E_{g,r}^{(z),act}(t) \right|^2} dt \tag{1}$$

where $\underline{x} = \{x_t,\, y_t,\, z_t,\, D_t,\, \varepsilon_t,\, \sigma_t\}$ is a vector of unknowns which define the characteristics of the malignant tissue, $E_{g,r}^{(z)}(\underline{x}, t)$ and $E_{g,r}^{(z)act}(t)$ are the time domain electric fields for the reference scenario and for a trial solution, collected at the receiving probe r when transmitting a pulse from probe g. The minimization of (1) is obtained by constructing a sequence of trial solutions with $k = 1, \ldots, K$, being k the iteration number, which converges toward the optimal solution $\underline{x}^{opt} = \arg\{\min[\Phi(\underline{x})]\}$.

3. THE BEE ALGORITHM

This section gives a brief description of the artificial bee colony optimizer and its customization to the problem at hand. A more detailed description of the algorithm can be found in the following references. Intelligent swarm-based optimization algorithms [27] such as Genetic Algorithm (GA) [19], Differential Evolution (DE) [21], Ant Colony Optimization (ACO) algorithm [28] and the Particle Swarm Optimizer (PSO) [22] algorithm, mimic behaviors seen in nature to drive a search towards the optimal solution in a multidimensional solution space. Thanks to their capabilities to avoid local minima, they have been efficiently used to solve complex practical problems, including microwave imaging problems. Recently a new intelligent swarm search algorithm, called the Artificial Bee Colony Algorithm (ABC), has been proposed for solving optimization problems [24]. The ABC algorithm is inspired by the food foraging behavior of swarms of honey bees and it seems to outperform other optimization techniques [29, 30]. In the ABC algorithm, the colony of artificial bees is composed of three groups of bees: employed bees, onlookers and

scouts. A bee waiting on the dance area to make a decision about choosing a food source, is called an onlooker, the bee going to the food source it visited previously is called an employed bee, and a bee carrying out a new random search is called a scout. In the following these three main processes, which govern the ABC algorithm, will be discussed. In order to describe the ABC algorithm, let us consider a colony Π of C bees

$$\Pi = \left\{ \underline{B}_o;\, o = 1, \ldots, O = \frac{C}{2} \right\} \cup \left\{ \underline{B}_e;\, e = 1, \ldots, E = \frac{C}{2} \right\} \tag{2}$$

where O and E are the number of onlooker and employed bees respectively. In this implementation we consider the first half of the colony as employed artificial bees and the second half as onlookers. For each employed bee a food source position, which represents a trial solution of the optimization problem, is defined as follows:

$$\underline{x}_k^e = \left\{ x_k^{e,j};\, j = 1, \ldots, J \right\} \tag{3}$$

where J is the number of unknowns, and k the iteration number. In the ABC algorithm, each cycle of the search consists of three steps: sending the employed bees to the food sources; measuring the amount of food; selecting the food sources investigated by the onlookers after sharing the information found by employed bees. The iterative procedure is summarized in the following:

- *Initialization.* A population of $X_k = \{x_k^e;\, e = 1, \ldots, \frac{C}{2}\}$ positions is randomly generated. As stated above a food position represents a trial solution of the optimization problem, and the amount of food corresponds to the fitness of the associated solution. The food positions are ranked according to their fitness value computed by considering the cost function for the problem at hand, $\phi_k^e = \phi\{\underline{x^e}_k\},\ e = 1, \ldots, \frac{C}{2}$. The employed bees then memorize the position of their specific food source, while the onlooker bees memorize all the food sources. The following steps will be iterated until the requirements are met.
- *Onlookers food source selections.* Onlookers select a food source by using a probability based process. For each food source they compute a probability value according the following relation:

$$p_e = \frac{\phi^e \left\{ \underline{x}_k^e \right\}}{\sum_{e=1}^{\frac{c}{2}} \phi \left\{ \underline{x}_k^e \right\}} \tag{4}$$

  where ϕ_k^e is the fitness of the e-th food source. each food source the associate onlooker bee chooses a source food h, from all the food sources, according the probability estimated with (4).

- *Employed bees food sources improvements.* To produce new food position from the old one, the employed bees use the following update equation:

$$x_{(k+1)}^{e,j} = x_k^{e,j} + R^{e,j}(x_k^{e,j} - x_k^{h,j}) \quad j = 1, \ldots, J \quad e = 1, \ldots, \frac{C}{2} \quad (5)$$

where e is the food source index, h is the source position chosen by the onlooker bee, and $R^{e,j}$ is a random number generator between 0 and 1.

- *Scouts explorations.* If a solution representing a food source is not improved after a predetermined maximum number of iterations ($L_{\max}$), then that food source is abandoned by its employed bee. The bee is converted into a scout which, is placed at a randomly generated new food source. $L_{\max}$ is known as the food source limit it is an important control parameter of the algorithm. A schematic which summarizes the algorithm is reported in Figure 2.

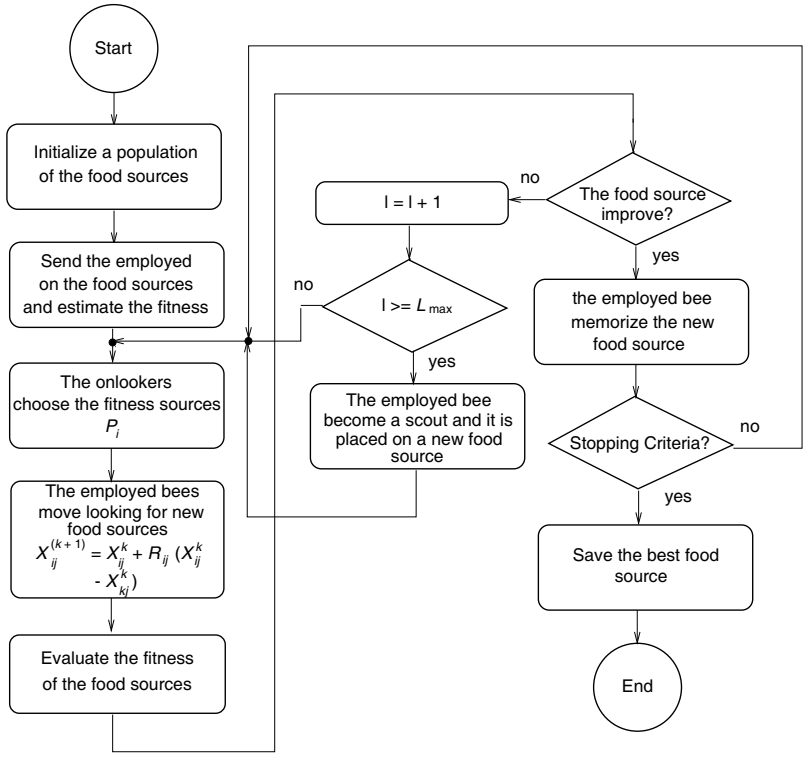

Figure 2. Flowchart of the artificial bee colony optimizer.

Table 1. Dielectric properties of the homogeneous breast tissue used in the considered three dimensional numerical model.

Tissue	ε	σ (S/m)
Coupling Liquid	9.0	0.200
Chest wall	20.0	0.297
Tumour	50.0	0.794
Normal Breast	20.0	0.297

4. NUMERICAL RESULTS

In this section the reconstruction methodology described in the previous section is assessed by numerical simulations. Three dimensional numerical breast models are considered. The investigation domain is a rectangular domain of $150 \times 150 \times 100\,\text{mm}^3$. The chest of the patient is simulated with a layer of thickness $T_c = 20\,\text{mm}$ and the breast is modeled with a hemisphere of diameter $2 * R_b = 150\,\text{mm}$. We assume the breast immersed in a coupling liquid ($\varepsilon_{back} = 9$, $\sigma_{back} = 0.2$) which completely fills the investigation scenario. The dielectric characteristics of the different components of the considered breast model are summarized in Table 1 and it is assumed that the dielectric characteristic of the tissues are constant in the whole frequency range of the considered interrogating pulse [31, 32].

A TLM-based solver [26] is used to produce synthetic measured and trial data. In order to avoid committing the inverse crime the measured field data for the direct problem is synthetically generated using a grid with cell size $\Delta x = \Delta y = \Delta z = 0.5\,\text{mm}$, the inverse problem is characterized with a grid size of $\Delta x = \Delta y = \Delta z = 0.7\,\text{mm}$. In particular the developed model consider 4.5 and 3.6 millions of cells for the direct and inverse problem respectively. The direct and inverse process considere 2000 time steps with a $\Delta t = 1.6 \times 10^{-12}\,\text{s}$. To limit the computational burden in all experiments we use only 5 views. For each view one probe is used as transmitter while the remaining 30 probes act as receivers, to collect the scattered data. In order to simulate a realistic environment, noise has been added to the numerical data, in particular an AWGN noise of SNR = 10 dB has been used [15, 16]. We consider the transmitter to be a point source, polarized along the z-axis, a single cycle sinusoid pulse with a 3 dB bandwidth of 3 GHz and a center frequency of 2 GHz has been used for the excitation Figure 3.

The parameters of the *ABC* were chosen after a calibration process, and the initial population chosen in a completely random

way. An optimum population of $C = 10$ bees have been considered (five onlookers and five employed chosen in a completely random way), and $L_{\max}$ was set to 5. Due to the high spatial resolution required, the computational burden of the three dimensional geometry being considered is quite high. For each view the time required to estimate the time domain scattering data on a personal computer equipped with an AMD Athlon (TM) 6000+ quad-core processor and 4 GB RAM is about 35 minutes. For the number of views and the

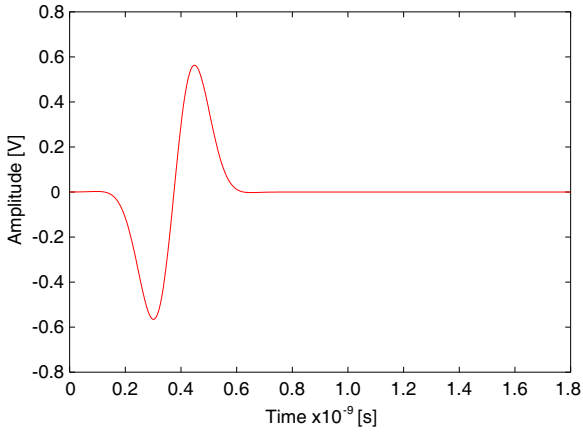

Figure 3. The wideband pulse adopted as source for generate the impinging electromagnetic field.

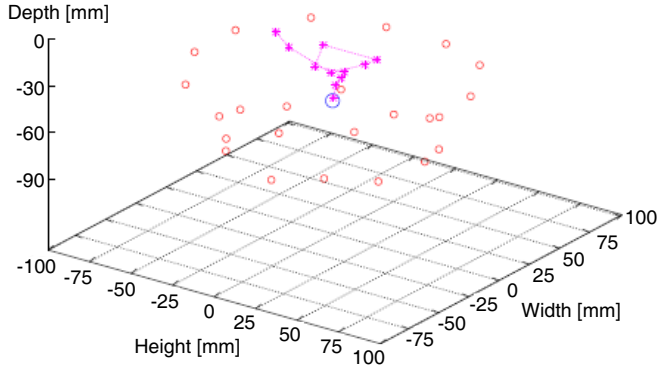

Figure 4. Reconstruction of the x, y, and z coordinates of the tumour center (coordinate of the best individual of the colony).

chosen population dimension, each iteration the inversion algorithm will take about 15 hours. In order to reduce the computational time the inversion procedure has been implemented as a parallel process following the guidelines reported in [25]. A cluster of five PC was used, reducing the computational time for a single iteration to about 3.75 hours. In the first example, we consider a breast model with a $D_t = 10\,\text{mm}$ diameter malignant inclusion of ($\varepsilon_t = 50$, $\sigma_t = 0.794$) placed at $x_t = y_t = 0\,\text{mm}$, $z_t = -51\,\text{mm}$. The reconstruction procedure described in the previous sections has been applied in order to localize the coordinates of the tumor center, the dimensions, and to reconstruct the dielectric parameters, which are important in order to identify the nature of the tissue. The iterative procedure reaches a stationary condition after about 20 iterations. The results are reported in Figures 4 and 5. Figure 4 shows the reconstruction of the tumor

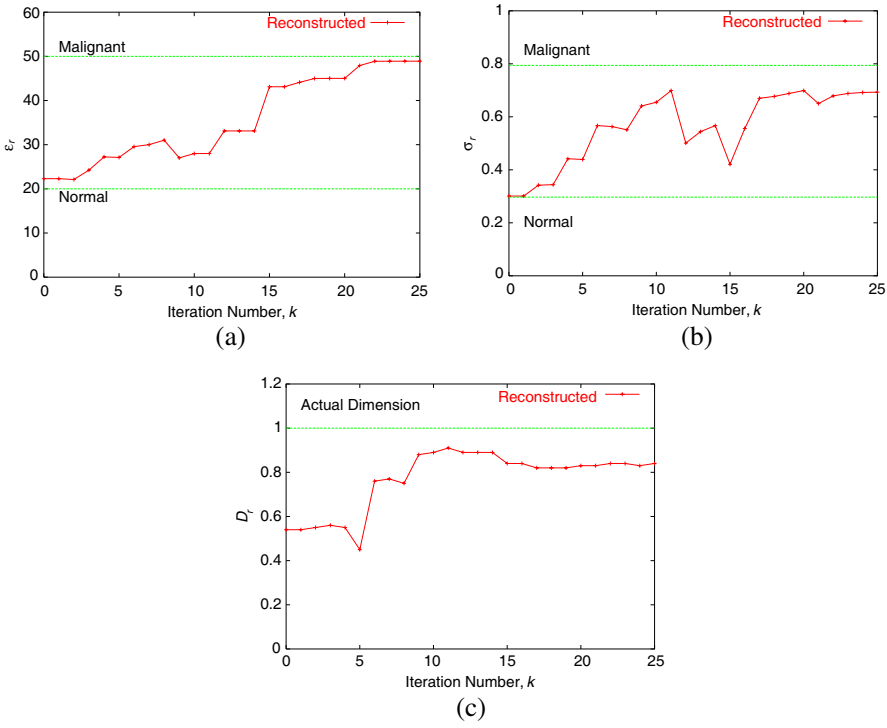

Figure 5. Reconstruction of the dielectric properties and the dimension of a centered homogeneous tumour obtained at the end of the minimization process. (a) Relative permittivity. (b) Conductivity, and (c) dimension.

center coordinates. The blue circle represents the actual coordinates of the tumor, and the red line the trajectory of the tumor center derived from the best solution of the colony during the minimization process. In Figure 4 it can be seen that after few iterations the tumor is located with a satisfactory degree of accuracy, although the starting point (completely randomly chosen) is rather distant from the exact position of the tumor. Figures 5(a) and (b) show the reconstructed values of the electric permittivity and conductivity versus the iteration number k. At the end of the minimization process the relative error is less than 5% for the conductivity and less than 6% for the permittivity. Also the estimation of the tumor dimension versus the iteration number, reported in Figure 5(c), is retrieved with a satisfactory degree of accuracy; at the end of the iterative procedure the relative error in the tumor size is less than 2 mm. In the second experiment, the diameter of the malignant inclusion is varied between 5 mm and 20 mm. While all other parameters are the same as in the previous experiment. Figure 6(a) shows the quantitative error in the reconstructed permittivity values χ_{eps} and conductivity χ_s. It can be seen that for inclusions above 10 mm the error is never greater than 10% in χ_{eps} and 15% for χ_s. While for smaller inclusions the error is no greater than 25%. Figure 6(b) shows the quantitative error in the tumor size and center position. Concerning the estimation of the tumor size we obtain an absolute error of about 3 mm for tumors with diameters from 10 mm up to 20 mm while for a diameter of 0.5 mm the absolute error fall down to 1 mm. The localization capabilities of the method are quite good, the coordinate of the tumor center are retrieved with an error less than 10% for all tumor dimensions. The estimation

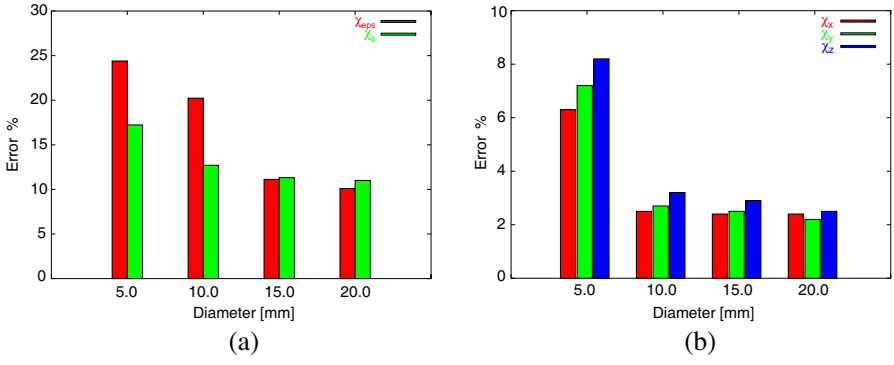

Figure 6. Reconstruction of a centered tumour, error figures versus dimension. (a) Quantitative, and (b) qualitative parameters.

Table 2. Breast model with a single malignant inclusions. comparisons of different stochastic optimizers.

	GA	PSO	DE	ABC
x_b	20.21	5.31	2.21	0.30
y_b	−25.32	20.21	−1.67	0.42
z_b	−14.51	−22.12	−20.21	−24.22
D_t	25.32	12.43	12.31	8.12
ε	38.21	41.23	41.30	48.81
σ	0.455	0.531	0.554	0.623

Table 3. Breast model with two inclusions. Localization, dimension estimation, and retrieved electric parameters of the malignant inclusion. The dimensions are in mm.

Tissues	x_b	y_b	z_b	D_t	ε	σ (S/m)
Actual Malignant	40.0	40.0	−30.0	10.0	50.0	0.794
Actual Fibro	20.0	20.0	−30.0	10.0	25.0	0.350
Retrieved Malignant	25.3	21.2	−24.3	23.1	40.1	0.604

of the tumor diameter is also satisfactory, the 20% error in the 5 mm reconstruction representing an absolute error of only 1 mm. For the sake of comparisons Table 2 shows the reconstructed parameters obtained by applying inversion procedure based on a standard genetic algorithm (GA), on a particle swarm (PSO) based procedure, and on the differential evolution (DE) based approach.

All the considered stochastic algorithms have been initialized with the same population consisting of 10 individuals, and the maximum number of considered iteration was fixed to $K = 25$. As far as the GA, PSO and DE parameters the following parameters configuration has been considered: $P_c = 0.9$ (crossover probability) and $P_m = 0.01$ (mutation probability) for the GA, $P_c = 0.5$ (crossover probability) and $Q = 0.8$ for the DE, $C_1 = C_2 = 2.0$ (acceleration terms) and $w = 0.4$ (constant inertial weight) for the PSO. The worst results are obtained by the GA algorithm which reach a stationary condition after about five iterations. The PSO and the DE obtain similar results, however as can be observed from the results reported in Table 2 the Bee algorithm outperforms the other considered stochastic algorithms. As the third and last example, we consider a breast model with two different inclusions, representing a malignant tumor and a benign inclusion, consisting of fibro glandular tissue. The two inclusions

have the same diameter of 10 mm, and they are separated by 10 mm. It is worth noticed that the proposed method is not able to detect multiple targets, we decide to consider this multi targets geometry for the sake of comparison and in order to show the limitation of the current version of the inversion procedure. The malignant tissue ($\varepsilon_t = 50$, $\sigma_t = 0.794$) and the fibro glandular inclusion ($\varepsilon_{fibro} = 25$, $\sigma_{fibro} = 0.25$) are placed at $x_t = y_t = 40\,\text{mm}$, $z_t = -30\,\text{mm}$ and $x_{fibro} = y_{fibro} = 20\,\text{mm}$, $z_{fibro} = -30\,\text{mm}$ respectively. Table 3 shows the qualitative and quantitative parameters reconstructed after the minimization procedure. It can be seen that as expected the method was not able to correctly identify the malignant tissues, in fact the reconstructed object has an area two times larger than the actual dimension of the malignant tissues and is located in the middle of the two inclusions, despite the not so high accuracy the method localized as malignant inclusion a spatial region very close to the real malignant tissue. To assess the capabilities of the proposed methodology in a realistic scenario, the last experiment deal with a realistic numerical breast phantom based on magnetic resonance images (MRI). In particular a numerical phantom characterized with less than 25% of glandular tissue, a Class 1 model according to the convention of the American College of Radiology, has been used. The phantom comes from the online database of anatomically realistic numerical breast phantoms provided by the University of Wisconsin Madison. In particular the ID = 071904 phantom, fibro-connettive tissues of class 1.2 and 1.3, and a cell size of $\Delta x = \Delta y = \Delta z = 0.5\,\text{mm}$ have been considered. Figure 7 shows the realistic three dimensional breast model, the blue dots represent the fibro-glandular tissue. To take into account the normal heterogeneous nature of the breast the electric characteristics of each cell representing the fibro-glandular tissue has been randomly chosen in the range $25 < \varepsilon < 30$ for the dielectric permittivity and $0.350 < \sigma < 0.450$ for the conductivity. As in the first example a single $D_t = 10\,\text{mm}$ diameter malignant inclusion of ($\varepsilon_t = 50$, $\sigma_t = 0.794$) placed at $x_t = y_t = 0$, $z_t = -51\,\text{mm}$ has been considered. The same algorithm parameters and the same cluster of machine of the previous experiments have been considered. At the end of the iterative procedure stopped after $K = 30$ iterations, the method identify an area of dimension $D_r = 20\,\text{mm}$ located at $x_r = -10\,\text{mm}$, $y_r = -15\,\text{mm}$, $z_r = -75\,\text{mm}$. As can be noticed the malignant inclusion has been localized and shaped with a satisfactory degree of accuracy. Also the retrieved electric characteristics ($\varepsilon_r = 38$, $\sigma_t = 520$) of the malignant inclusion are retrieved with a satisfactory degree of accuracy despite the heterogeneous structure of the breast. Also in this example the method is able to identify with a reasonable

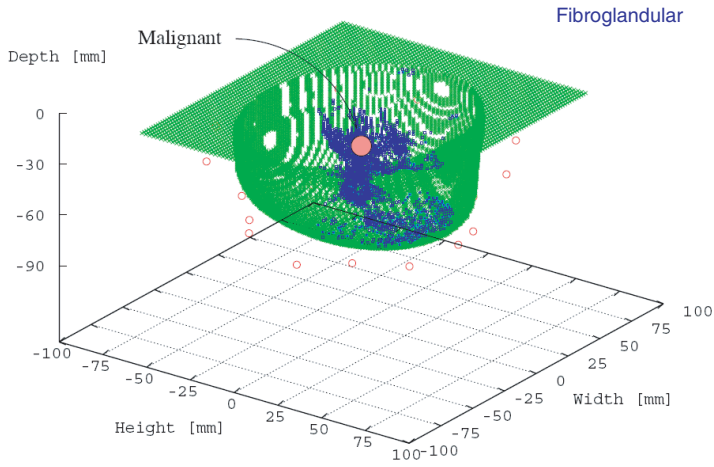

Figure 7. The three dimensional realistic numerical breast model based on real MRI data. The green and blue dots show the asimmetric breast geometry and the fibroglandular/fibroconnective inclusions respectively.

degree of accuracy the malignant tissue, however the sospicious area is very close to the actual position of the malignant inclusion. It is hoped that by combining this approach with a clustering methods [33] and a gradient based solver (in order to enhance the convergence ratio) the inversion procedure will be able to resolve and correctly identify the malignant tissue. However it is worth noticed that due to the no free lunch theorem [34] one can customize an algorithm or a given methodology in order to obtain superior results only for a class of problems, a superior method able to works on the class of all possible problems do not exist.

5. CONCLUSION

A microwave imaging method was used to successfully detect tumors embedded in a simple breast model. The time domain inversion problem has been solved by defining a suitable cost function minimized by means of an efficient evolutionary algorithm, namely the artificial bee colony optimizer. The results demonstrate the potential of the proposed method in a simplified as well as realistic breast imaging scenario. Future work will be devoted to extend the method to imaging not only to the reconstruction of the malignant tissue characteristics, but also to the reconstruction to the breast characteristics in more

realistic phantoms.

ACKNOWLEDGMENT

The authors wish to thank E. Zastrow, S. K. Davis, M. Lazebnik, F. Kelcz, B. D. Van Veen, and S. C. Hagness of the University of Wisconsin Madison, for kindly provide the online repository of anatomically realistic numerical breast phantoms.

REFERENCES

1. Tang, J., R. M. Rangayyan, J. Xu, I. El Naqa, and Y. Yang, "Computer-aided detection and diagnosis of breast cancer with mammography: Recent advances," *IEEE Trans. Inf. Technol. Biomed.*, Vol. 13, No. 2, 236–251, 2009.
2. Fang, Q., P. Meaney, T. Raynolds, C. Foxm, Q. Fang, et al., "Initial clinical experience with microwave breast imaging in woman with normal mammography," *Academic Radiology*, Vol. 14, No. 2, 207–218, 2007.
3. O'Halloran, M., E. Jones, and M. Glavin, "Quasi-multistatic MIST beamforming for the early detection of breast cancer," *IEEE Trans. Biomed. Eng.*, Vol. 57, No. 4, 830–840, 2010.
4. Klemm, M., I. J. Craddock, J. A. Leendertz, A. Preece, and R. Benjamin, "Radar-based breast cancer detection using a hemispherical antenna array experimental results," *IEEE Trans. Antennas Propagat.*, Vol. 57, No. 6, 1692–1704, 2009.
5. Kurrant, D. J. and E. Fear, "An improved technique to predict the time-of-arrival of a tumor response in radar-based breast imaging," *IEEE Trans. Biomed. Eng.*, Vol. 56, No. 9, 1200–1209, 2009.
6. Li, X., S. Hagness, D. B. Van Deen, and D. Van Den Weide, "Experimental investigation of microwave imaging via space-time beamforming for breast cancer detection," *Proc. IEEE International Microwave Symposium*, Vol. 1, 379–382, 2003.
7. Bond, E. J., X. Li, S. C. Hagness, and B. D. Van Veeenm, "Microwave imaging via space-time beamforming for early detection of breast cancer," *IEEE Trans. Antennas Propagat.*, Vol. 51, No. 8, 1690–1705, 2003.
8. Fear, E. C., X. Li, S. C. Hagness, and M. A. Stuchly, "Confocal microwave imaging for breast cancer detection: Localization of tumors in three dimensions," *IEEE Trans. Biomed. Eng.*, Vol. 49, No. 8, 812–822, 2002.

9. Nilavalan, R., I. J. Craddock, A. Preece, J. Leendertz, and R. Benjamin, "A wideband planar antenna for in-body imaging," *IEEE AP-S International Symposium and USNC/URSI National Radio Science Meeting*, Washington DC, Jul. 2005.
10. Klemm, M., J. A. Leendertz, D. Gibbins, I. Craddock, A. Preece, and R. Benjamin, "Microwave radar-based breast cancer detection: Imaging in inhomogeneous breast phantoms," *IEEE Antennas and Wireless Propagation Letters*, Vol. 8, 1349–1352, 2009.
11. Chen, Y., I. Craddock, P. Kosmas, M. Ghavami, and P. Rapajic, "Multiple-input multiple-output radar for lesion classification in ultrawideband breast imaging," *IEEE Journal of Signal Processing*, Vol. 4, No. 1, 187–201, 2010.
12. Rubk, T., P. M. Meaney, P. Meincke, and K. D. Paulsen, "Nonlinear microwave imaging for breast-cancer screening using GaussNewton's method and the CGLS inversion algorithm," *IEEE Trans. Antennas Propagat.*, Vol. 55, No. 8, 2320–2331, 2007.
13. Meaney, P., M. W. Fanning, R. M. Di Florio-Alexander, P. A. Kaufman, S. D. Geimer, T. Zhou, and K. D. Paulsen, "Microwave tomography in the context of complex breast cancer imaging," *2010 Annual International Conference of the IEEE Engineering in Medicine and Biology Society (EMBC)*, 3398–3401, 2010.
14. Fang, Q., P. Meaney, S. Geimer, A. Streltsov, and K. Paulsen, "Microwave image recostruction from 3-D field coupled to 2-D parameter estimation," *IEEE Trans. Biomed. Eng.*, Vol. 23, No. 4, 475–484, 2004.
15. Johnson, J. E., T. Takenaka, and T. Tanaka, "Two-dimensional time-domain inverse scattering for quantitative analysis of breast composition," *IEEE Trans. Biomed. Eng.*, Vol. 55, No. 8, 1941–1945, 2008.
16. Johnson, J. E., T. Takenaka, and T. Tanaka, "Experimental three-dimensional time-domain reconstruction of dielectric objects for breast cancer detection," *Proc. Mediterr. Microw. Symp.*, 423–426, 2006.
17. Johnson, J. E., T. Takenaka, K. A. Hong Ping, S. Honda, and T. Tanaka, "Advances in the 3-D forward-backward time-stepping (FBTS) inverse scattering technique for breast cancer detection," *IEEE Trans. Biomed. Eng.*, Vol. 56, No. 9, 2232–2243, 2009.
18. Zhou, H., T. Takenaka, J. Johnson, and T. Tanaka, "A breast imaging model using microwaves and a time domain three dimensional reconstruction method," *Progress In Electromagnetics Re-*

search, Vol. 93, 57–70, 2009.

19. Samii, Y. R. and E. Michielssen, *Electromagnetic Optimization by Genetic Algorithms*, Wiley, New York, 1999.
20. Rocca, P., M. Benedetti, M. Donelli, D. Franceschini, and A. Massa, "Evolutionary optimization as applied to inverse scattering problems," *Inverse Problems*, Vol. 12, No. 25, 1999.
21. Donelli, M., A. Massa, G. Oliveri, M. Pastorino, and A. Randazzo, "A differential evolution based multi-scaling algorithm for microwave imaging of dielectric structures," *Proceedings of IEEE International Conferences on Imaging Systems and Techniques, IST 2010*, 90–95, 2010.
22. Donelli, M. and A. Massa, "Computational approach based on a particle swarm optimizer for microwave imaging of two-dimensional dielectric scatterers," *IEEE Transactions on Microwave Theory and Techniques*, Vol. 53, No. 5, 1761–1776, 2005.
23. Donelli, M., G. Franceschini, A. Martini, and A. Massa, "An integrated multiscaling strategy based on a particle swarm algorithm for inverse scattering problems," *IEEE Transactions on Geoscience and Remote Sensing*, Vol. 44, No. 2, 298–312, 2006.
24. Tereshko, V. and A. Loengarov, "Collective decision-making in honey bee foraging dynamics," *Computing and Information Systems Journal*, Vol. 9, No. 3, 1352–9404, ISSN, 2005.
25. Massa, A., D. Franceschini, G. Franceschini, M. Pastorino, M. Raffetto, and M. Donelli, "Parallel GA-based approach for microwave imaging applications," *IEEE Trans. Antennas Propagat.*, Vol. 53, No. 10, 3118–3127, 2005.
26. Hoefer, W. J., "The transmission-line matrix method-theory and applications," *IEEE Transactions on Microwave Theory and Techniques*, Vol. 33, 882–893, 1985.
27. Bonabeau, E., M. Dorigo, and G. Theraulaz, *Swarm Intelligence: From Natural to Artificial Systems*, Oxford University Press, New York, 1999.
28. Rocca, R., L. Manica, F. Stringari, and A. Massa, "Ant colony optimisation for tree-searching-based synthesis of monopulse array antenna," *Electronics Letters*, Vol. 44, No. 13, 783–785, 2008.
29. Karaboga, D. and B. Basturk, "A Powerful and efficient algorithm for numerical function optimization: Artificial Bee Colony (ABC) algorithm," *Journal Global Optim. Mathematics and Computation*, Vol. 214, 108–132, 2009.
30. Karaboga, D. and B. Akay, "A comparative study of artificial

bee colony algorithm," *Journal Applied Mathematics and Computation*, Vol. 214, 108–132, 2009.

31. Zastrow, E., S. K. Davis, M. Lazebnik, F. Kelcz, B. D. Van Veen, and S. C. Hagness, "Development of anatomically realistic numerical breast phantoms with accurate dielectric properties for modeling microwave interactions with the human breast," *IEEE Trans. Biomed. Eng.*, Vol. 55, No. 12, 2792–2800, 2008.
32. Lazebnik, M., D. Popovic, L. McCartney, C. B. Watkins, M. J. Lindstrom, J. Harter, S. Sewall, T. Ogilvie, A. Magliocco, T. M. Breslin, W. Temple, D. Mew, J. H. Booske, M. Okoniewski, and S. C. Hagness, "A large scale study of the ultrawideband microwave dielectric properties of normal, benign, and malignant breast tissues obtained from cancer surgeries," *Phys. Med. Biol.*, Vol. 52, 6093–6115, 2007.
33. Caorsi, S., M. Donelli, and A. Massa, "Detection, location and imaging of multiple scatterers by means of the iterative multiscaling method," *IEEE Transactions on Microwave Theory and Techniques*, Vol. 52, No. 4, 1217–1228, 2004.
34. Wolpert, D. H. and W. G. Macready, "No free lunch theorems for optimization," *IEEE Trans. Evolutionary Computations*, Vol. 1, 67–82, 1997.